Supporting Information for

Rapid Formation of Antifouling Coatings via Cation-π Interactions

Zhicheng Huang, [a] *Kaijie Zhao,* [a] *Shaoyin Wei,* [a] *Yingxin Hao,* [a] *Qina Yu,* [a] *Jingcheng Hao,* [a] *Jiwei Cui,* [a] *Peiyu Zhang* [a,*]

[a] Key Laboratory of Colloid and Interface Chemistry of the Ministry of Education, School of Chemistry and Chemical Engineering Shandong University Jinan, Shandong 250100, P. R. China

[*] E-mail: Peiyu Zhang: pyzhang@sdu.edu.cn

Materials

Poly(ethylene glycol) methyl ether methacrylate (PEGMA), methacryloxyethyltrimethyl ammonium chloride (METAC), and 4-Cyano-4-(phenylcarbonothioylthio)pentanoic acid (CAPDB) were sourced from Meryer (Shanghai) Chemical Technology Co., Ltd. 2,2'-Azobis(2-methylpropionitrile) (AIBN), deuterium oxide, ethyl alcohol, and ethyl ether were procured from Shanghai Macklin Biochemical Technology Co., Ltd. Tannic acid (TA) was obtained from Sigma-Aldrich, while iron(II) chloride tetrahydrate was acquired from Shanghai D&B Biotechnology Co., Ltd. Silicon (Si) wafers were purchased from Tebo Technology Co., Ltd. Gold (Au) chips were supplied by RenLux Crystal Co., Ltd. (China). Dulbecco's modified Eagle's medium (DMEM, High Glucose) was purchased from Beijing Neuronbc Laboratories Co., Ltd. (China). Fetal bovine serum (FBS) was obtained from Gibco (Germany). Human umbilical vein endothelial cells (HUVEC) were sourced from the Cell Bank of the Chinese Academy of Sciences (Shanghai, China). Escherichia coli (E. coli) was obtained from the China General Microbiological Culture Collection Center. Biovision and Calcein-AM were purchased from Dalian Meilun Biotechnology Co., Ltd. (China). SYTO 9 and Trypticase (Tryptic) Soy Broth Medium were procured from Thermo Fisher Scientific. Ultrapure water was produced using a Milli-Q ultrapure water system with a resistivity of 18.2 MΩ cm^{-1}.

Biocompatibility Testing

HUVEC cells were cultured in high-glucose DMEM supplemented with 10% FBS and 1% penicillin/streptomycin at 37 °C in a 5% CO_2 incubator. The cytotoxicity of the different polymeric coatings was evaluated using MTT and live/dead staining assays. Following copolymer modification, the 24-well plates were sterilized using UV light for 30 min. The copolymer-modified 24-well plates were then incubated in high-glucose DMEM supplemented with 10% FBS and 1% penicillin/streptomycin for 24 h, after which the copolymer soak solution was prepared. HUVEC cells were seeded into a 96-well plate at a density of 1×10^4 cells $well^{-1}$ and co-incubated with 50% and 100% concentrations of copolymer extract for 24 h. Then, 10 μL of MTT solution (5 mg mL^{-1}) was added to each well and incubated for 4 h. The culture medium was subsequently removed, and 100 μL of DMSO was added to dissolve the formazan produced. The absorbance at 570 nm was measured using a microplate reader. In addition, HUVEC cells were seeded in a 24-well plate at a density of 1×10^5 cells $well^{-1}$ and co-incubated with the copolymer coating for 24 h. The medium was then replaced with 500 μL of PBS containing Calcein-AM (2 μM) and propidium iodide (4 μM) and incubated for 10 min. Live/dead cells were imaged using an inverted fluorescence microscope.

Platelet Adhesion

To obtain platelet-rich plasma (PRP), fresh rat blood was taken by venipuncture of a sole healthy individium and centrifuged at 1500 rpm for 10 min. The adhesion of platelets was assessed using copolymer-modified cell culture slides. The series of

culture slides were immersed in PRP, keeping at 37 °C. After 4 h of incubation, unattached platelets were gently rinsed with PBS. The attached platelets were observed using a microscopy, and the number of platelets in the microscopy images was quantified using ImageJ software. All animal experiments were approved by the Animal Ethics Committee of Shandong University (22012).

Statistical Analysis

All experimental data were presented as mean ± standard deviation (SD). Differences between groups were analyzed using Student's t-test. P-values less than 0.05 were considered statistically significant.

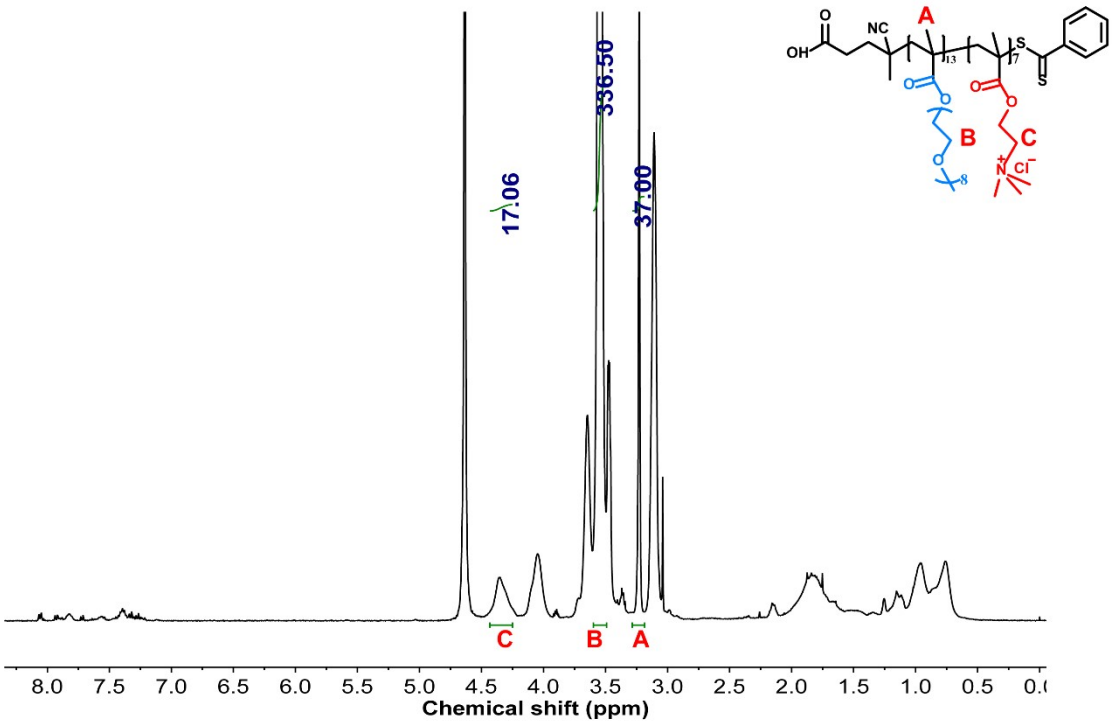

Figure S1. ^{1}H NMR (400 MHz, D_2O) spectra of r-P_{13}-M_7.

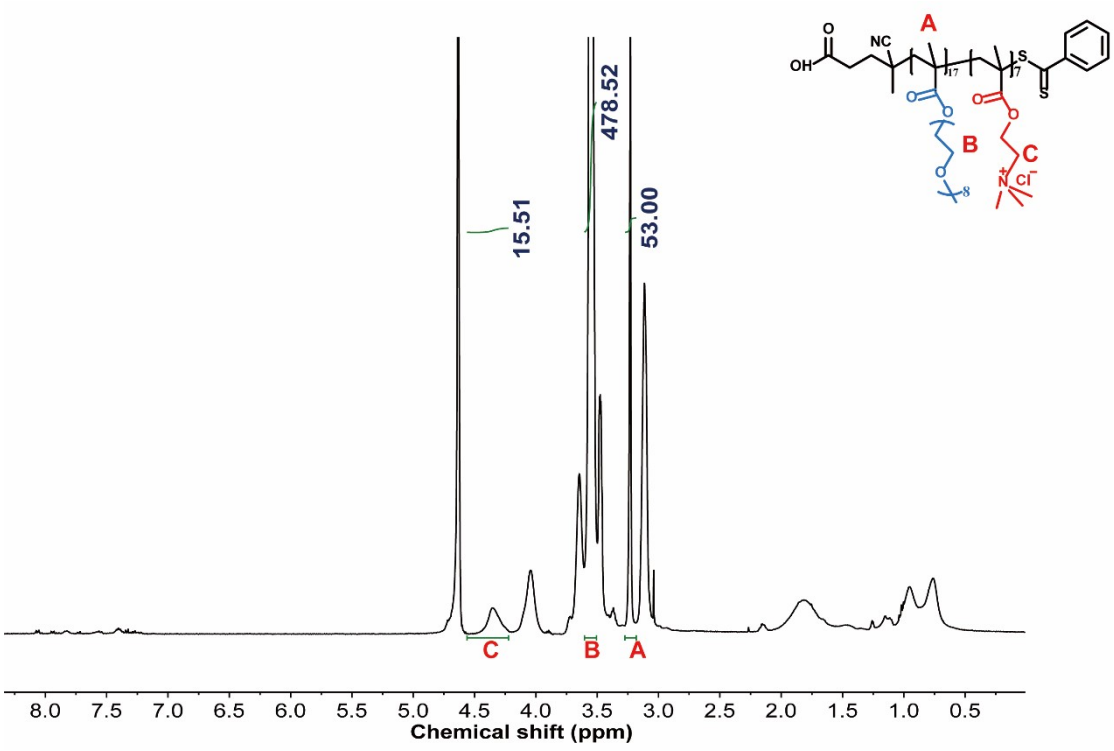

Figure S2. ^{1}H NMR (400 MHz, D_2O) spectra of r-P_{17}-M_7.

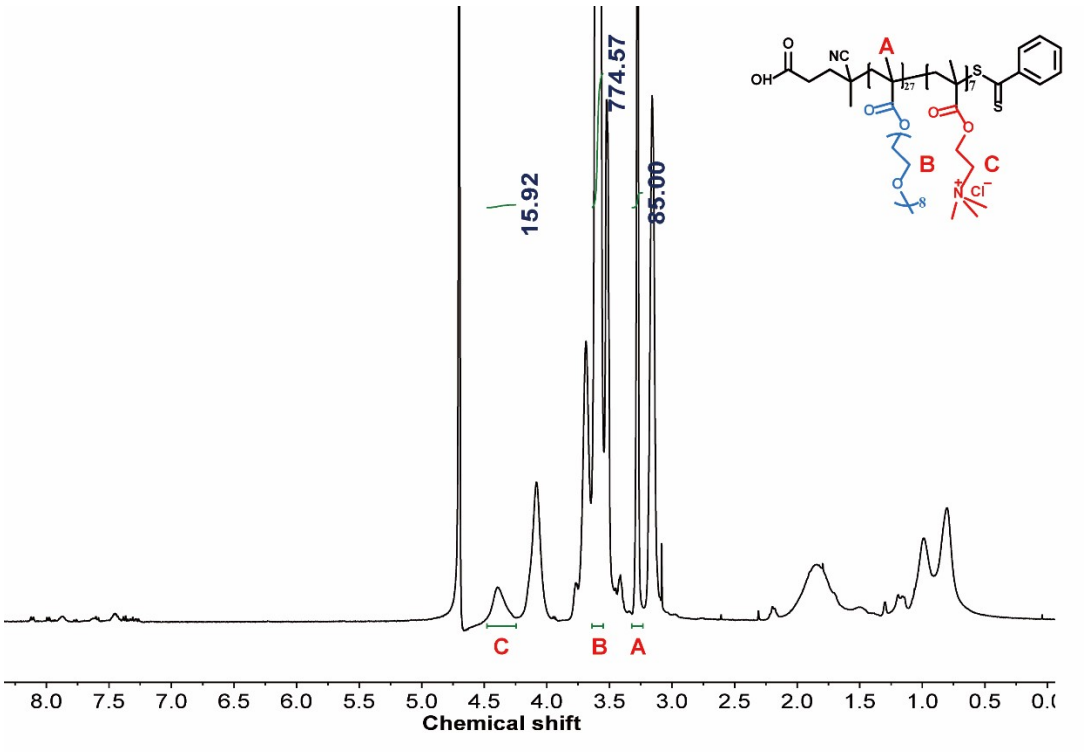

Figure S3. ^{1}H NMR (400 MHz, D_2O) spectra of r-P_{27}-M_7.

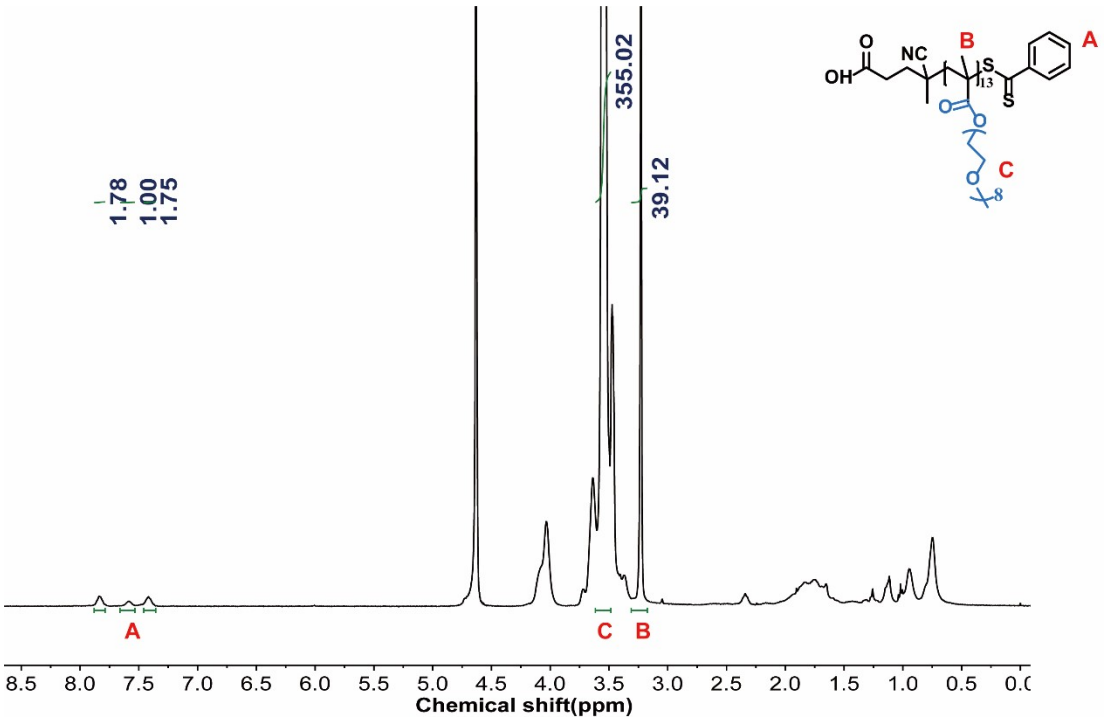

Figure S4. ^{1}H NMR (400 MHz, D_2O) spectra of PEG_{13}.

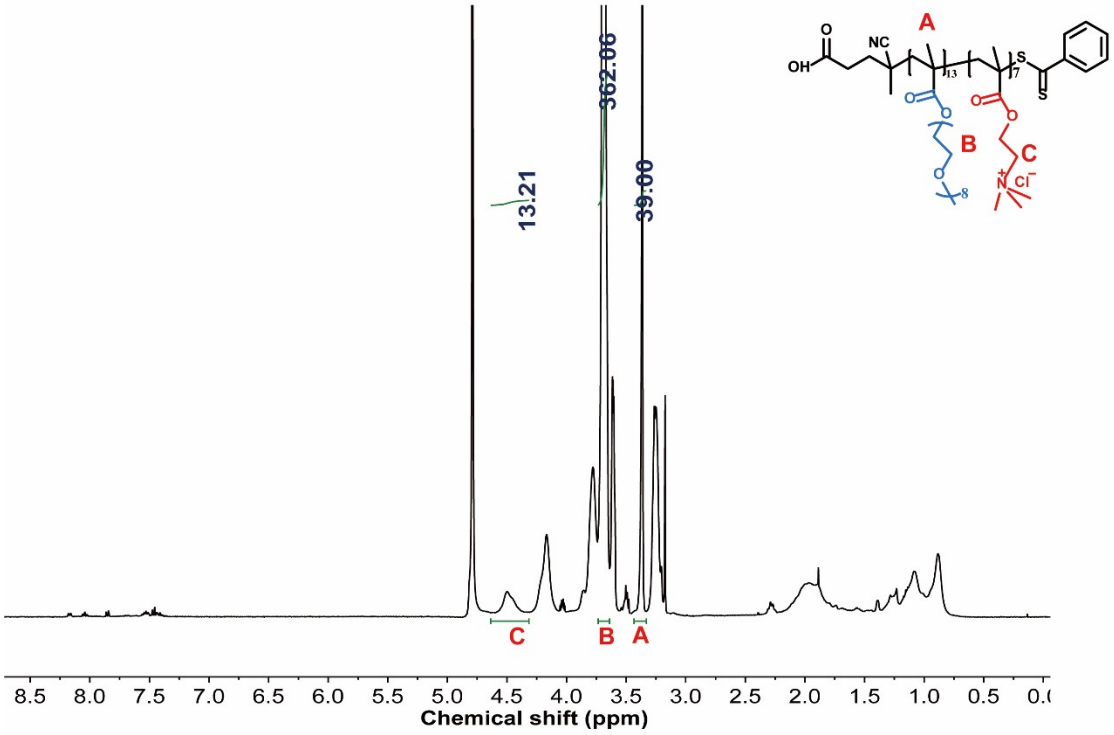

Figure S5. ^{1}H NMR (400 MHz, D_2O) spectra of bl-P_{13}-M_7.

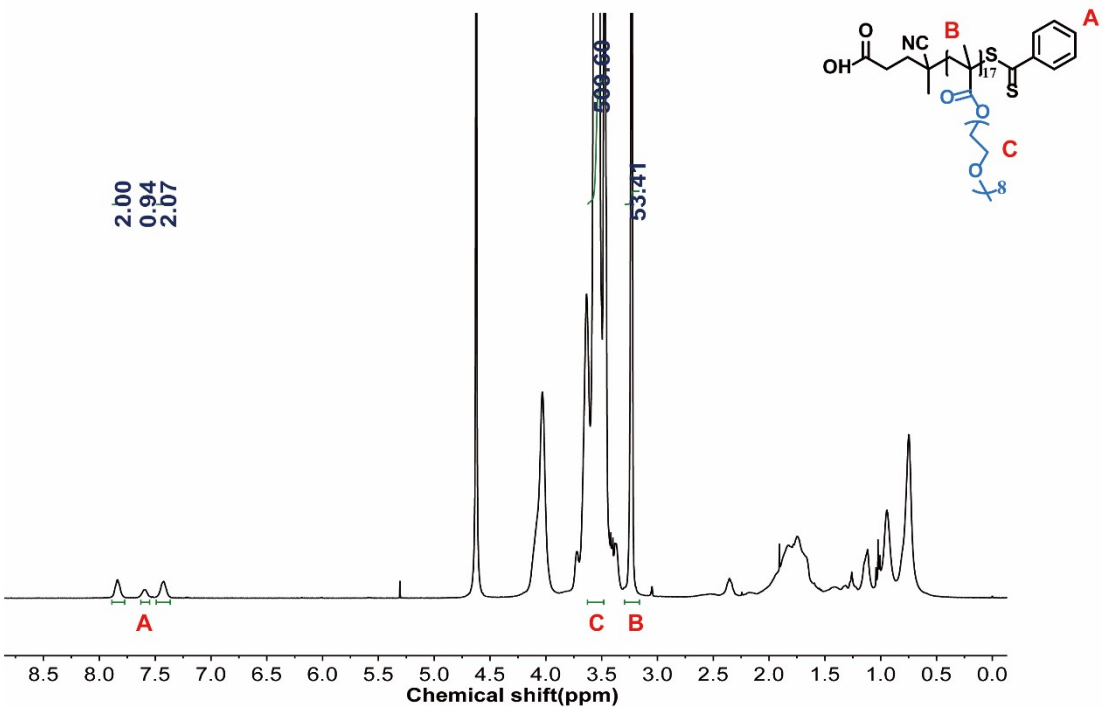

Figure S6. ^{1}H NMR (400 MHz, D_2O) spectra of PEG_{17}.

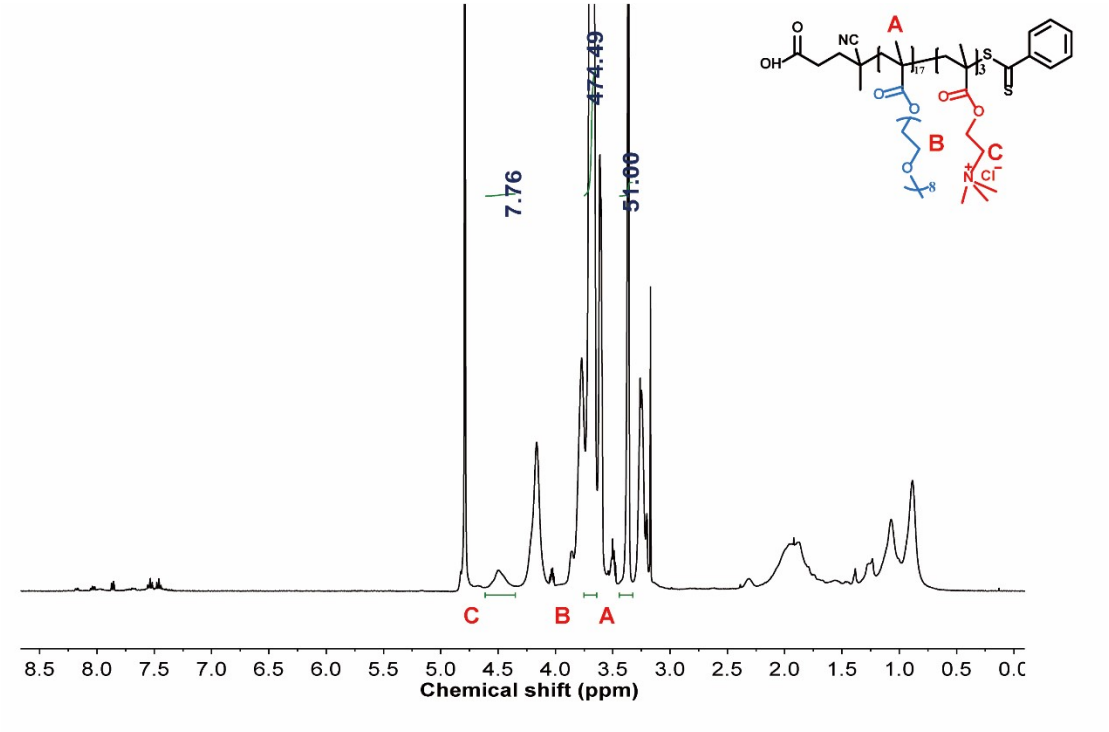

Figure S7. ^{1}H NMR (400 MHz, D_2O) spectra of bl-P_{17}-M_3.

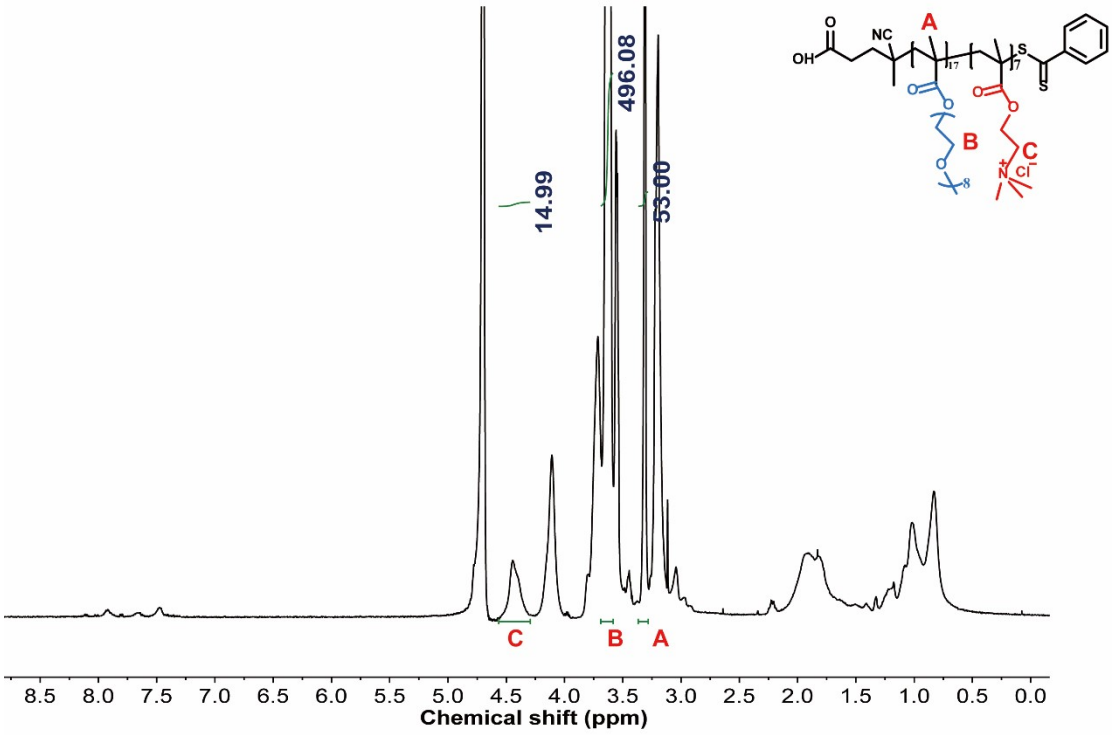

Figure S8. ^{1}H NMR (400 MHz, D_2O) spectra of bl-P_{17}-M_7.

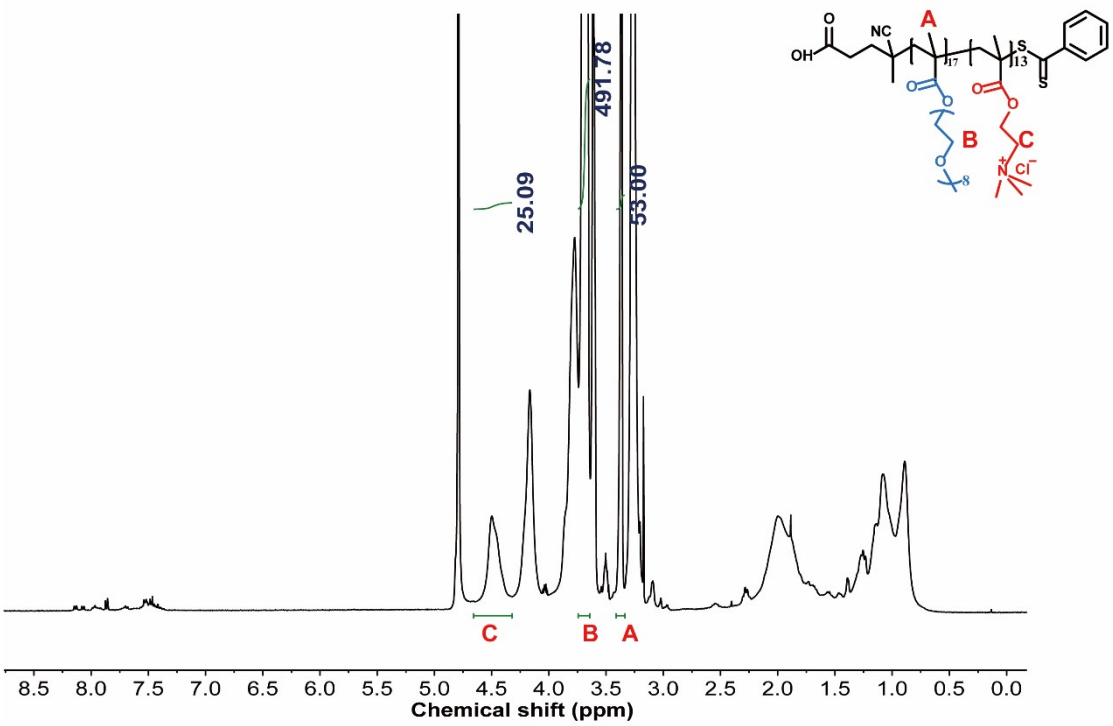

Figure S9. ^{1}H NMR (400 MHz, D_2O) spectra of bl-P_{17}-M_{13}.

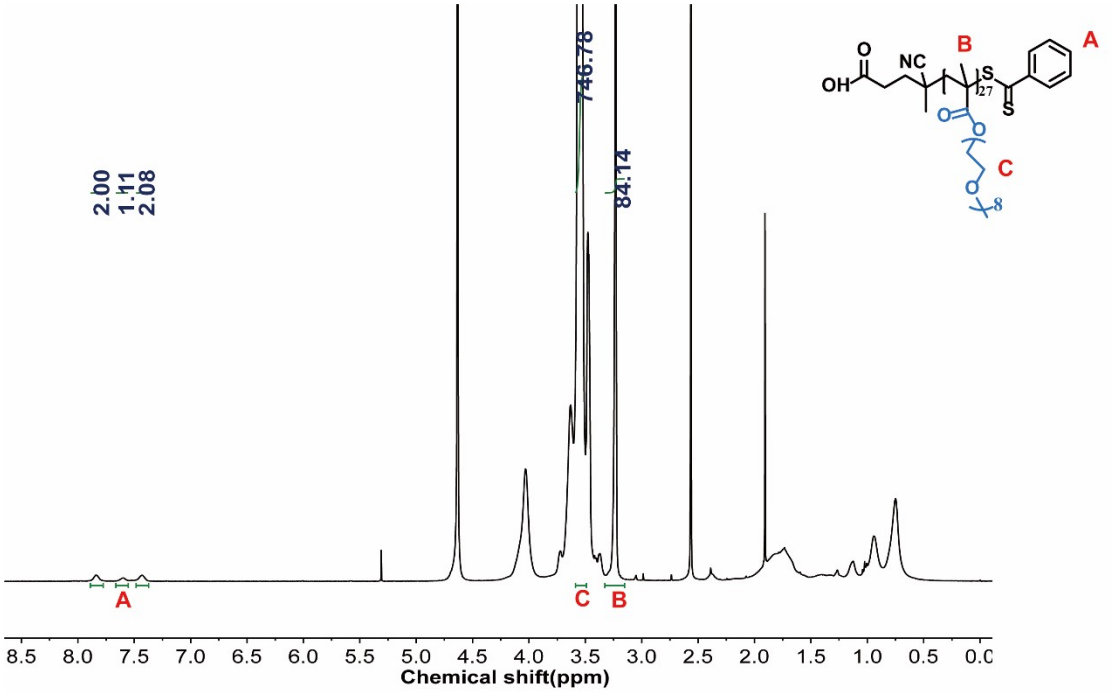

Figure S10. ^{1}H NMR (400 MHz, D_2O) spectra of PEG_{27}.

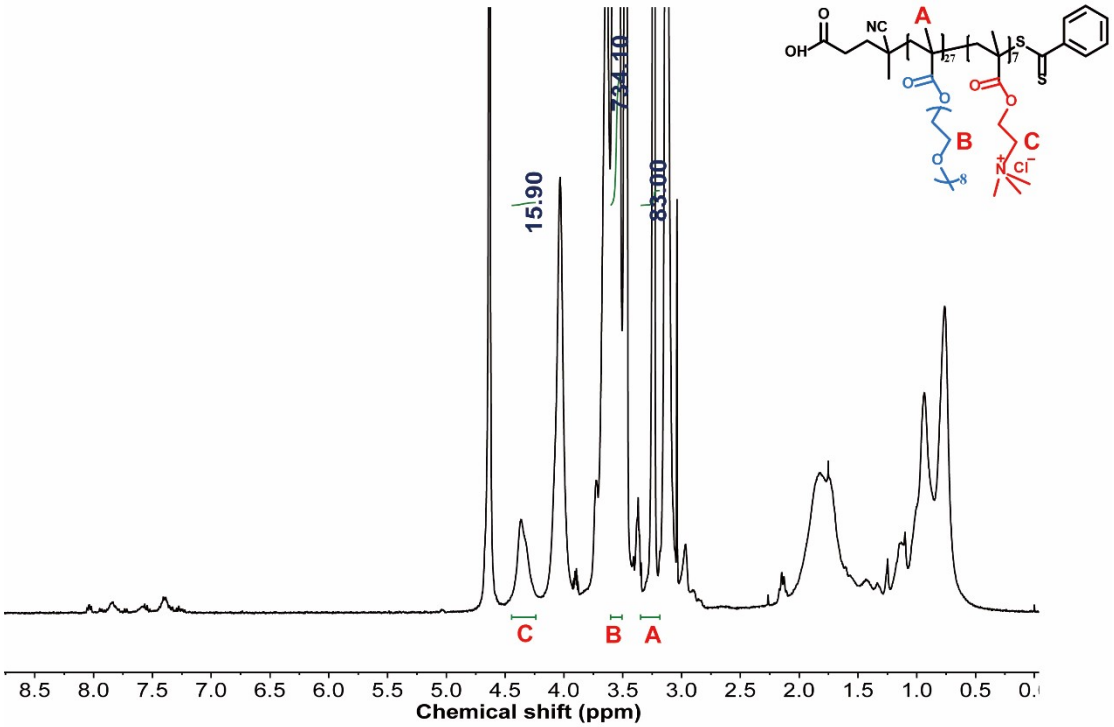

Figure S11. ^{1}H NMR (400 MHz, D_2O) spectra of bl-P_{27}-M_7.

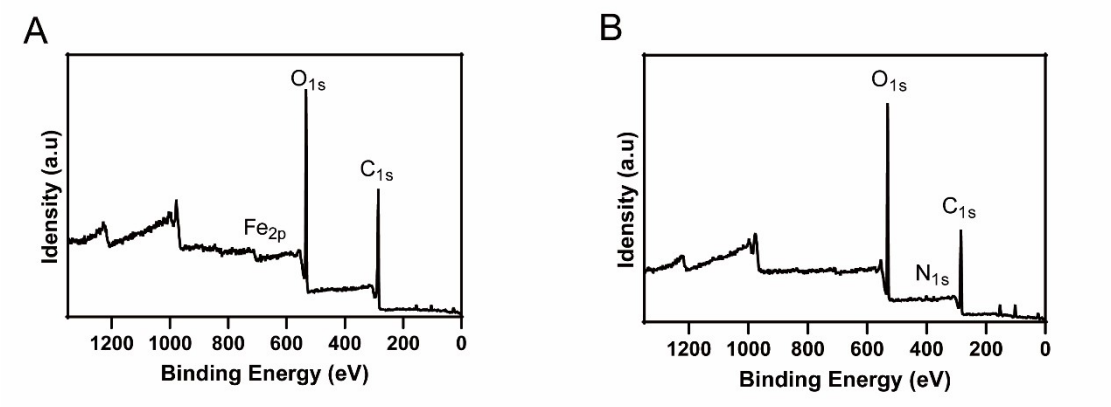

Figure S12. (A) XPS on slides modified with MPN. (B) XPS on slides modified with MPN and copolymer.

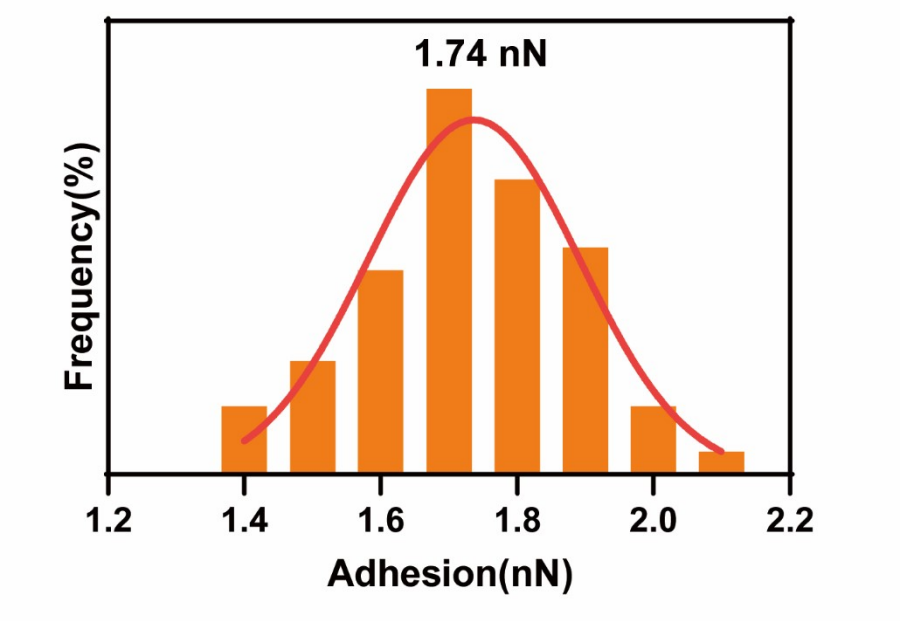

Figure S13. The adhesion force between the tip and coating.

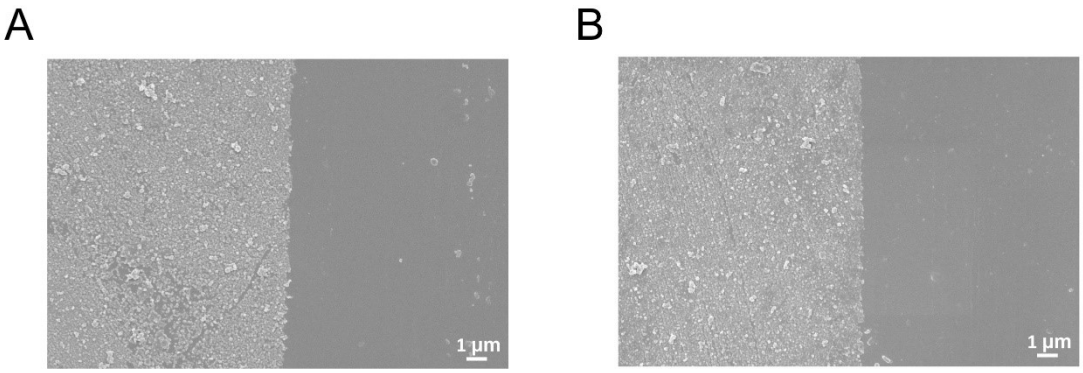

Figure S14. (A) SEM images of coatings. (B) SEM images of coatings after adhesion with 3M tape.

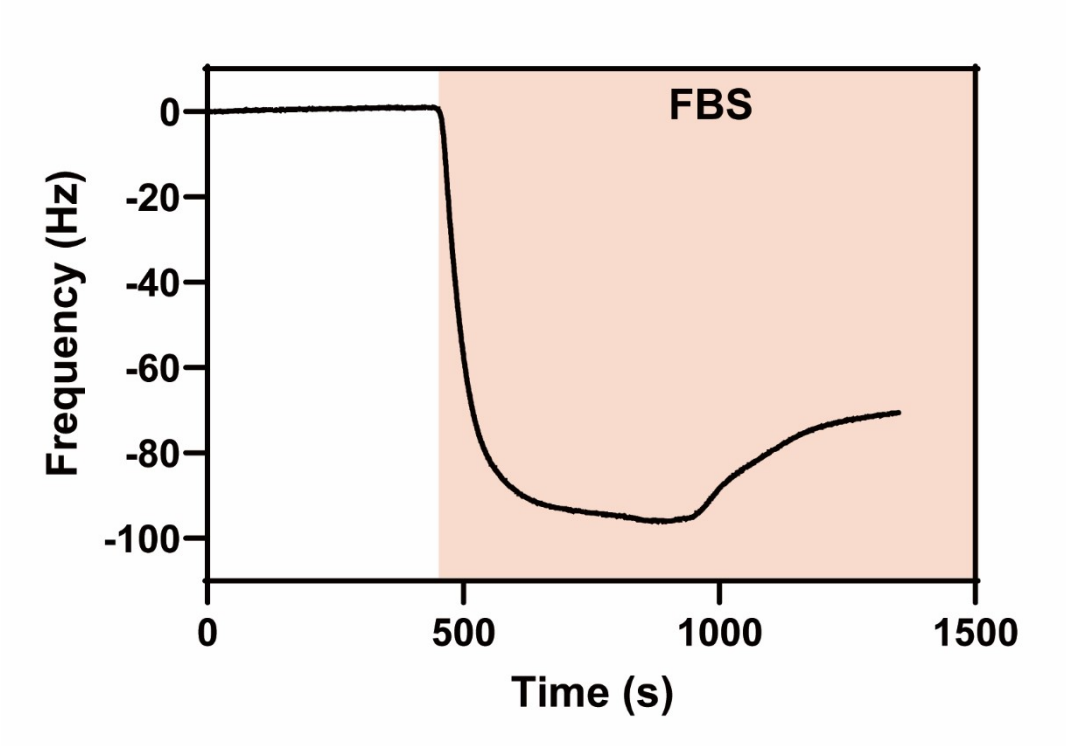

Figure S15. QCM-D frequency changes for FBS adsorption on Au chips.

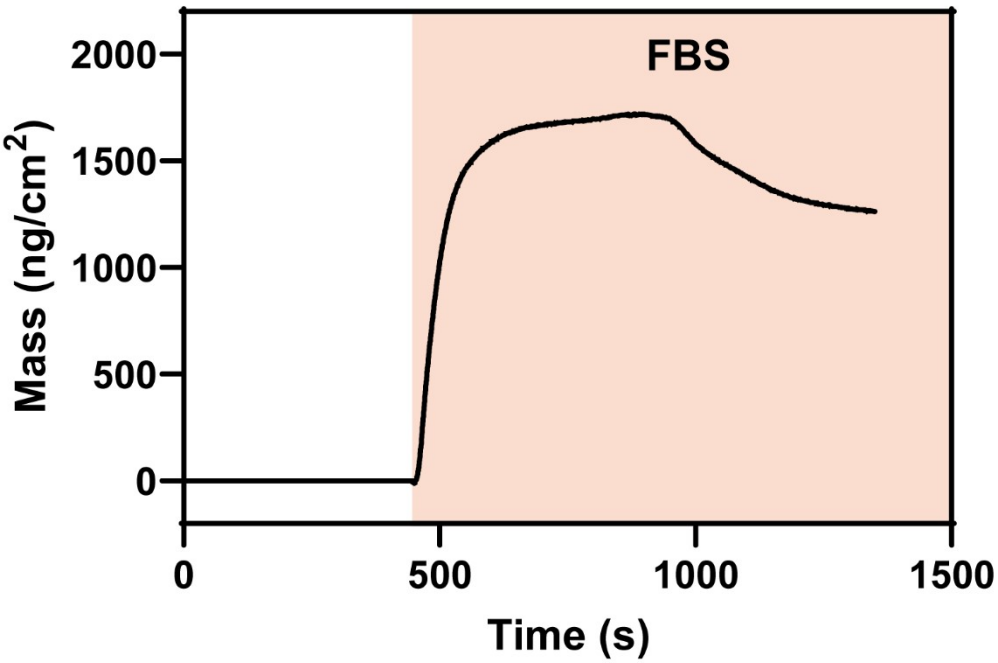

Figure S16. QCM-D mass changes for FBS adsorption on Au chips.

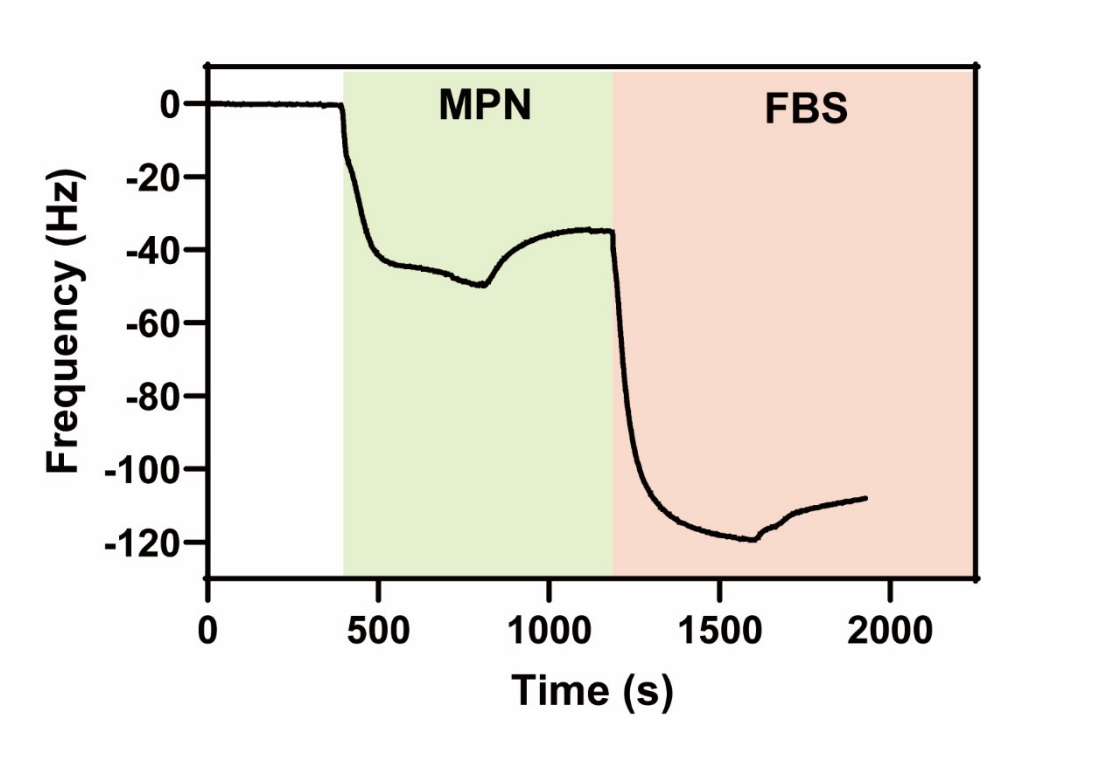

Figure S17. QCM-D frequency changes of copolymer modified Au substrates after FBS adsorption of MPN.

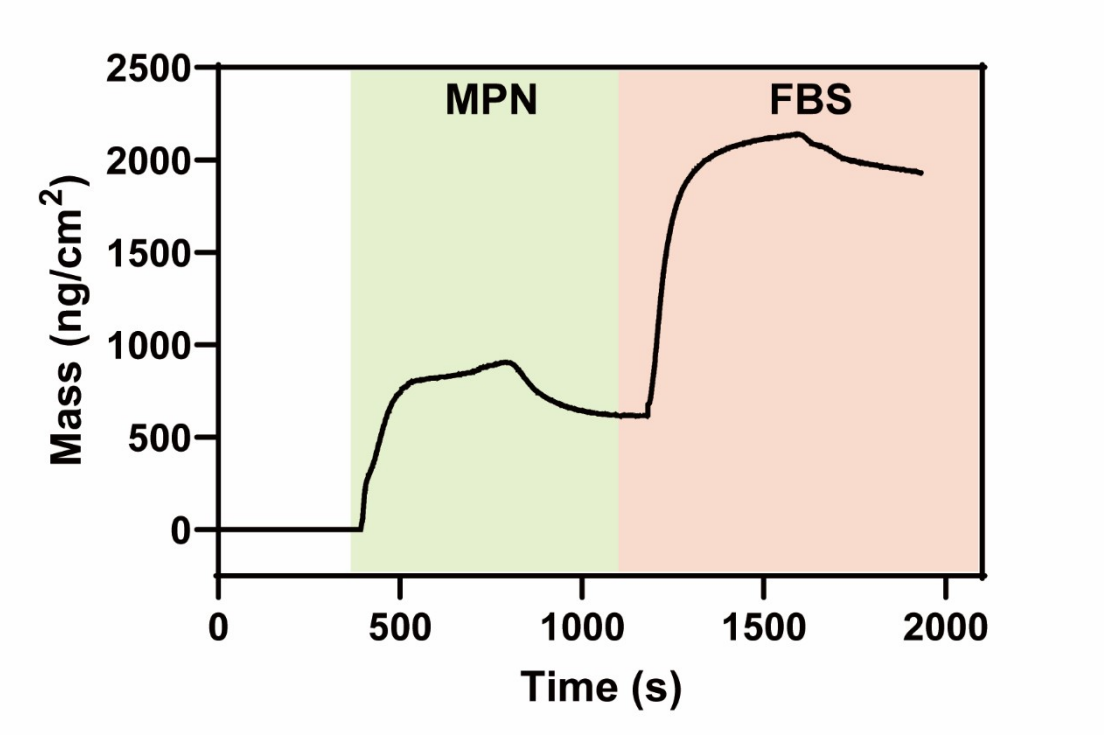

Figure S18. QCM-D mass changes of copolymer modified Au substrates after FBS adsorption of MPN.

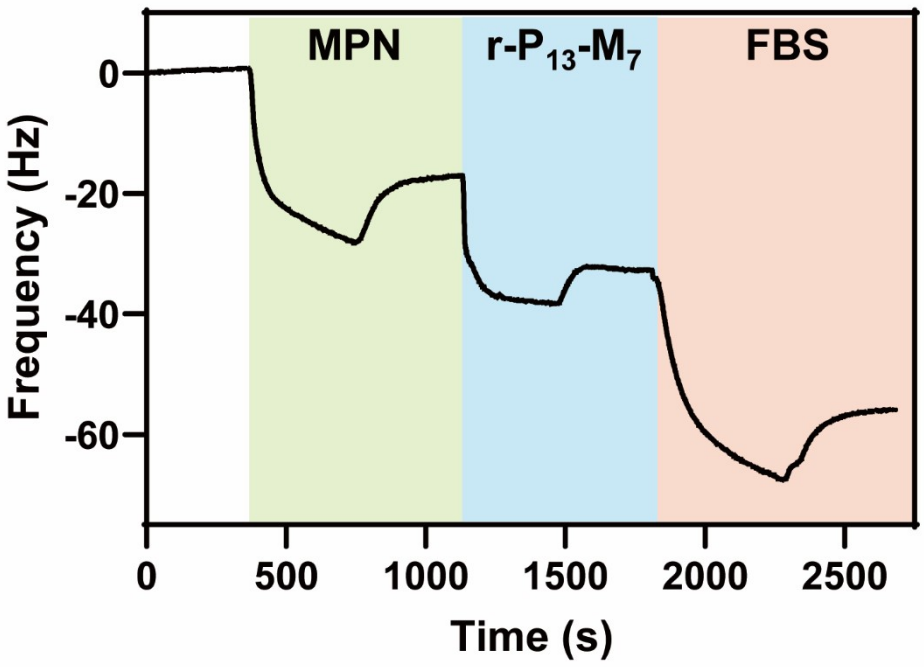

Figure S19. QCM-D frequency changes of copolymer modified Au substrates after FBS adsorption of r-P_{13}-M_7.

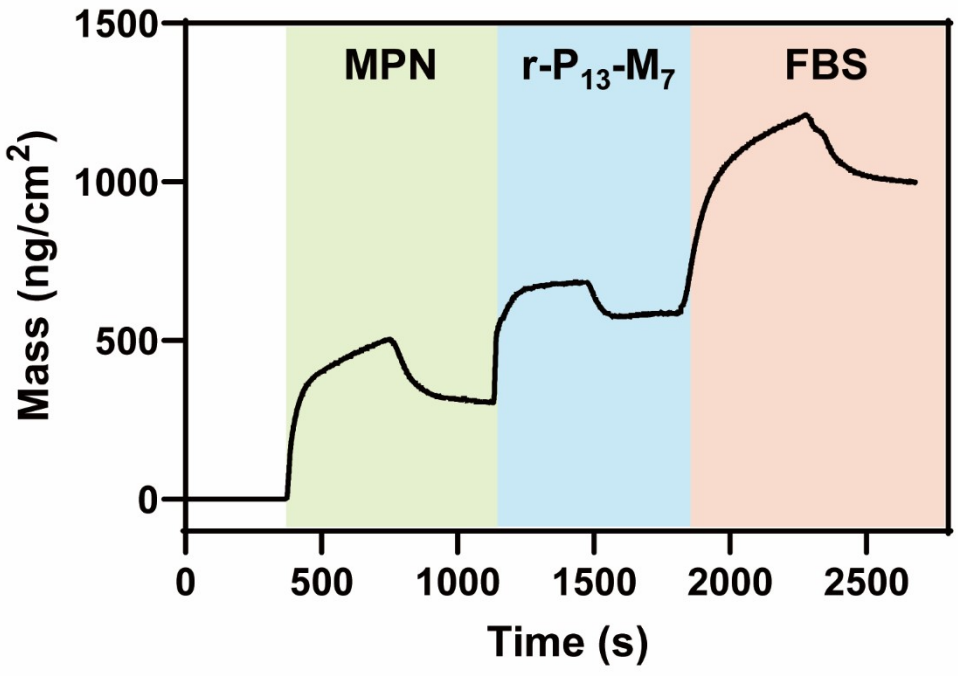

Figure S20. QCM-D mass changes of copolymer modified Au substrates after FBS adsorption of r-P_{13}-M_7.

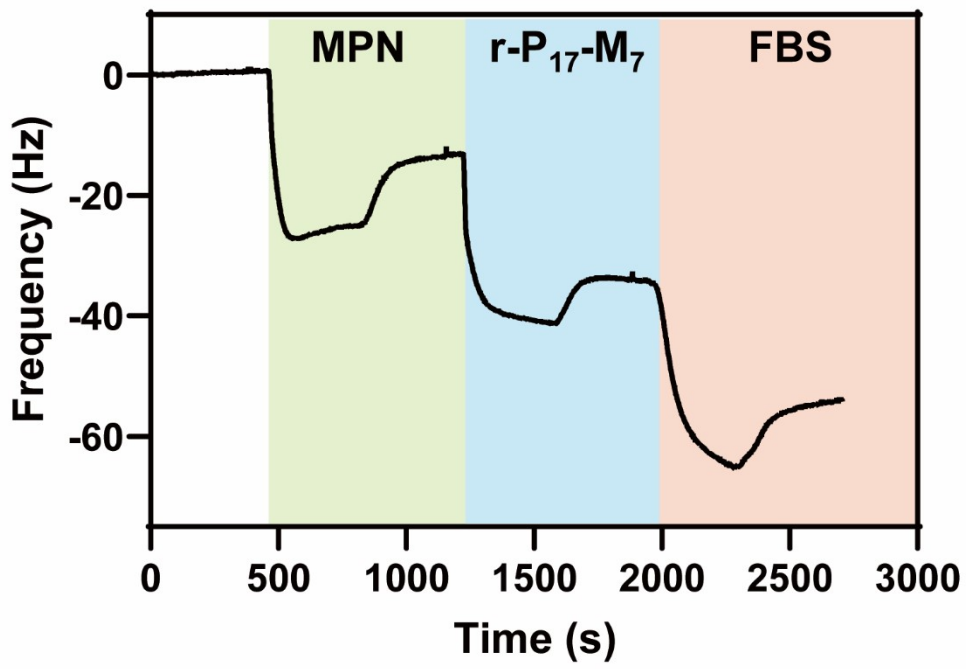

Figure S21. QCM-D frequency changes of copolymer modified Au substrates after FBS adsorption of r-P_{17}-M_7.

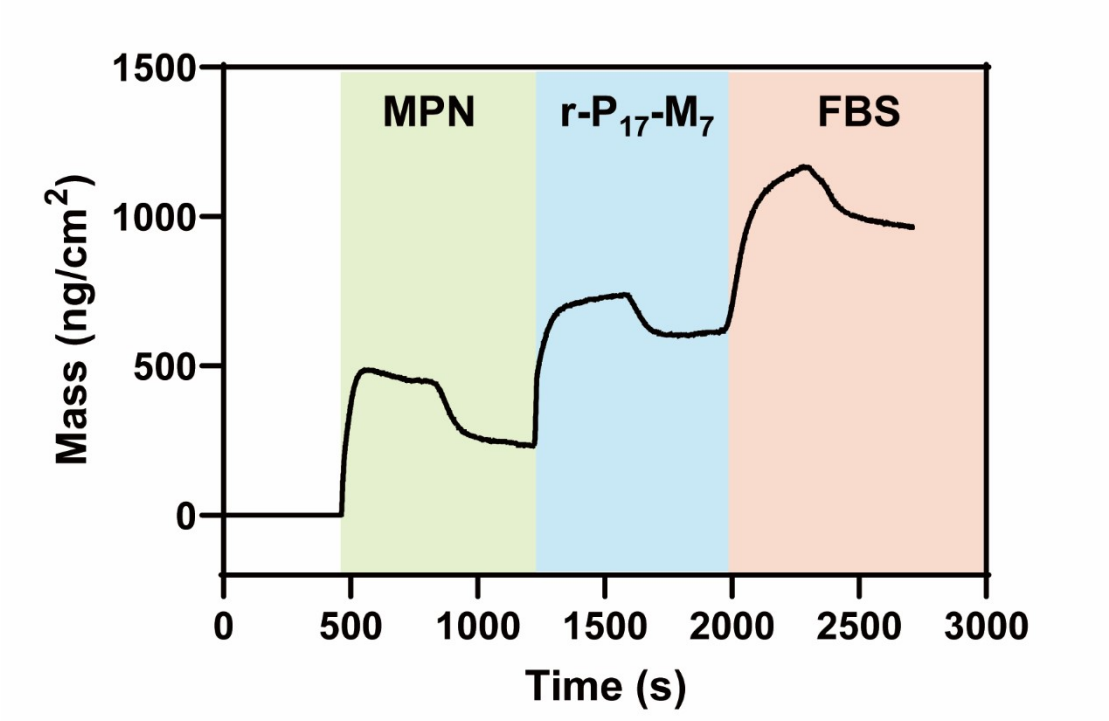

Figure S22. QCM-D mass changes of copolymer modified Au substrates after FBS adsorption of r-P_{17}-M_7.

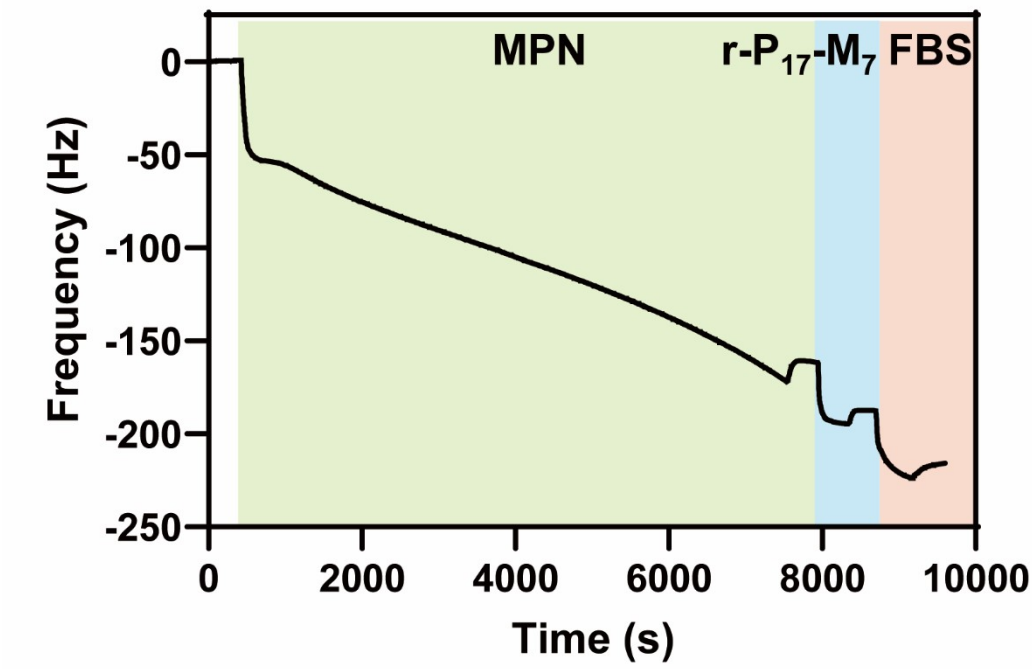

Figure S23. QCM-D frequency changes of copolymer modified Au substrates after FBS adsorption of r-P_{17}-M_7-2h.

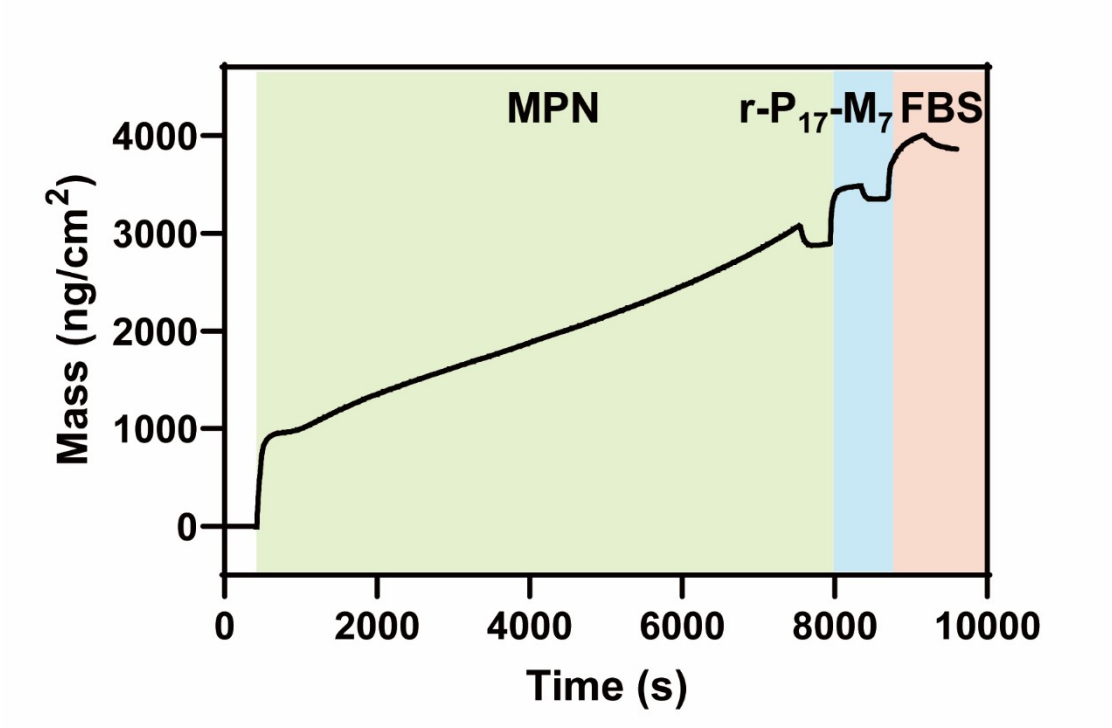

Figure S24. QCM-D mass changes of copolymer modified Au substrates after FBS adsorption of r-P_{17}-M_7-2h.

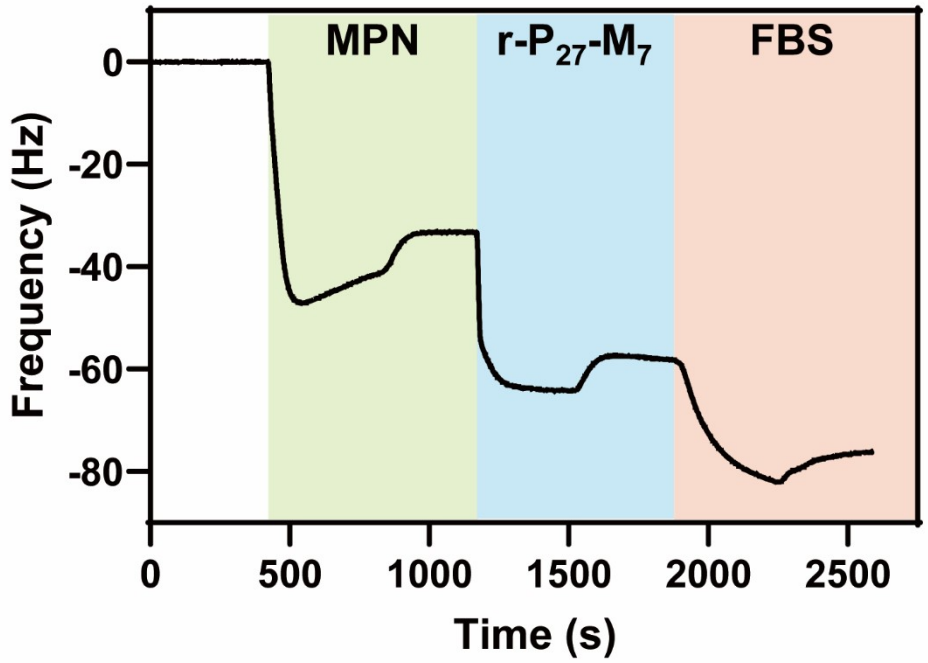

Figure S25. QCM-D frequency changes of copolymer modified Au substrates after FBS adsorption of r-P_{27}-M_7.

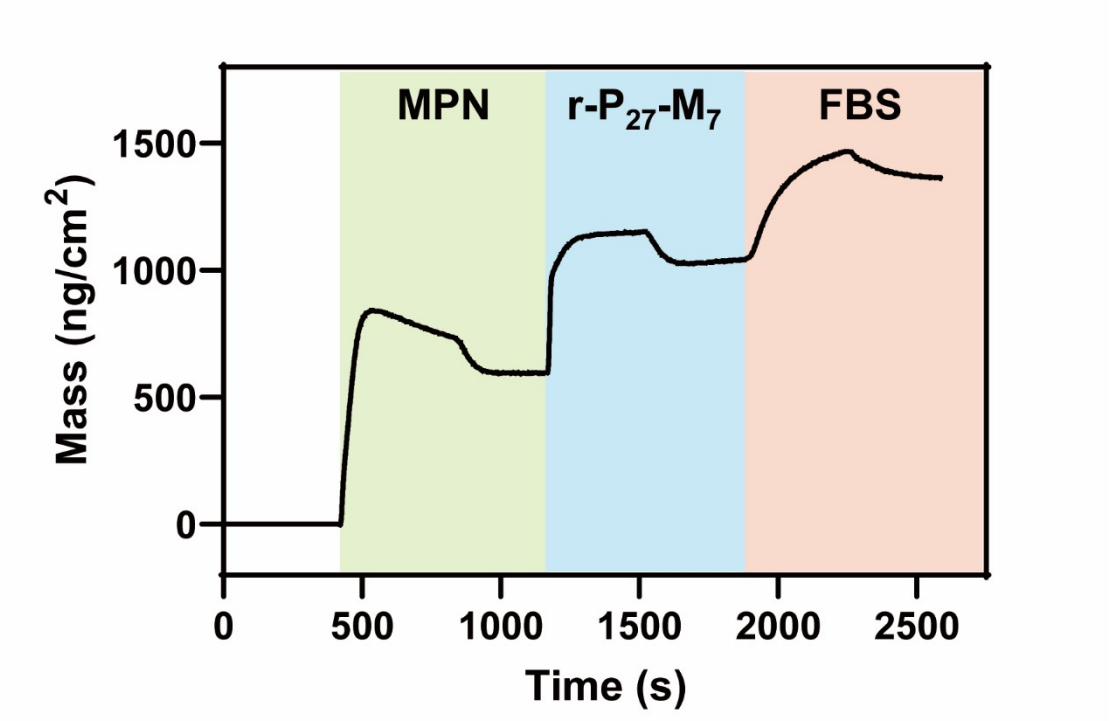

Figure S26. QCM-D mass changes of copolymer modified Au substrates after FBS adsorption of r-P_{27}-M_7.

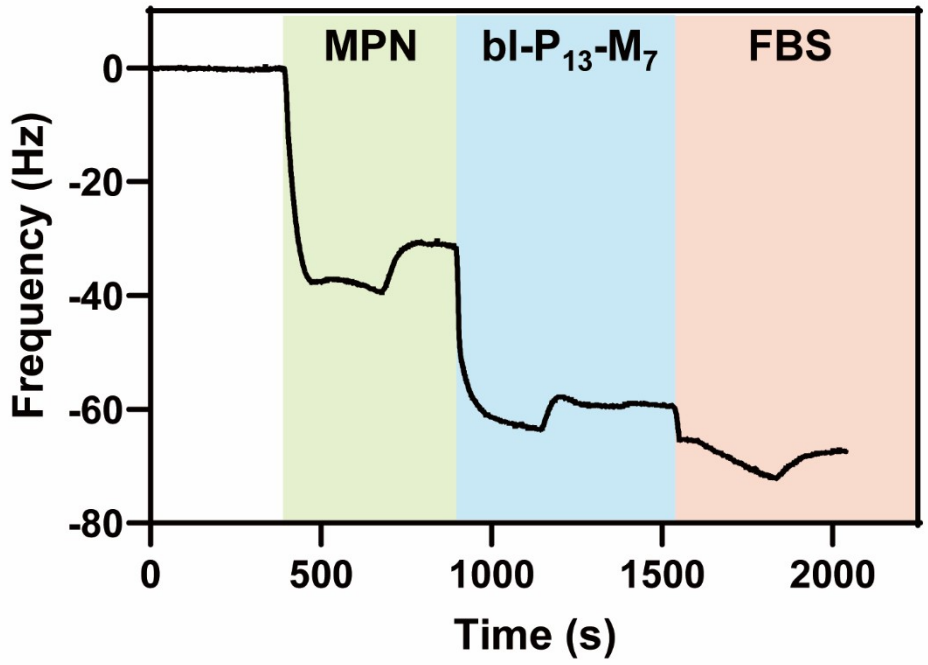

Figure S27. QCM-D frequency changes of copolymer modified Au substrates after FBS adsorption of bl-P_{13}-M_7.

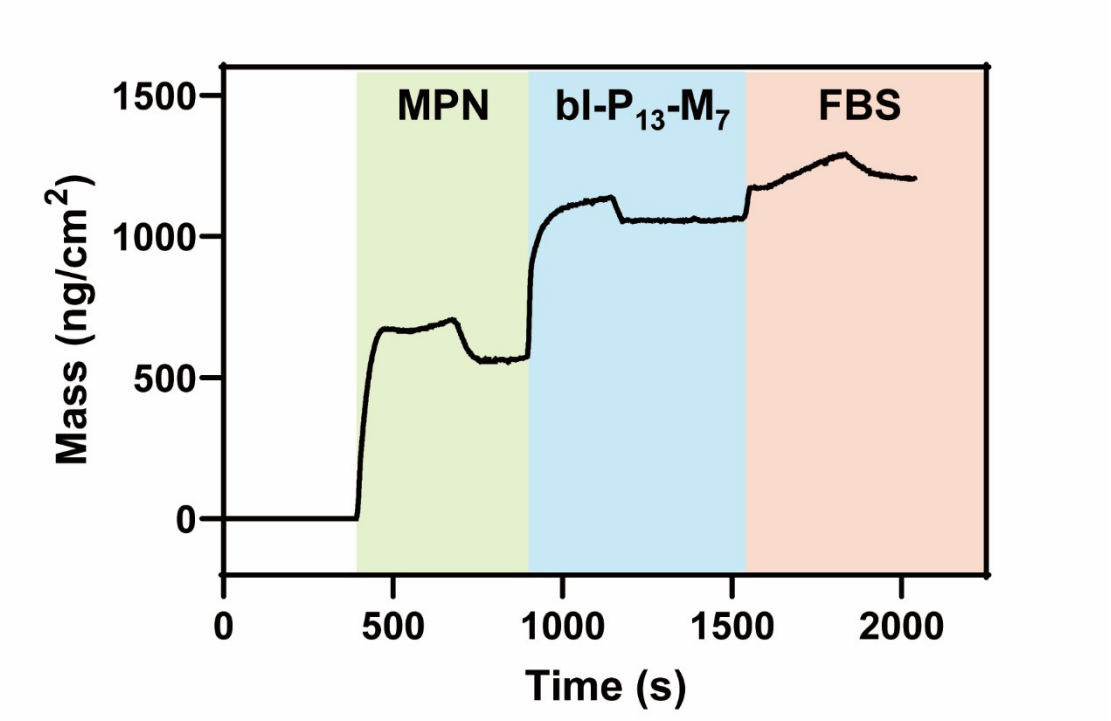

Figure S28. QCM-D mass changes of copolymer modified Au substrates after FBS adsorption of bl-P_{13}-M_7.

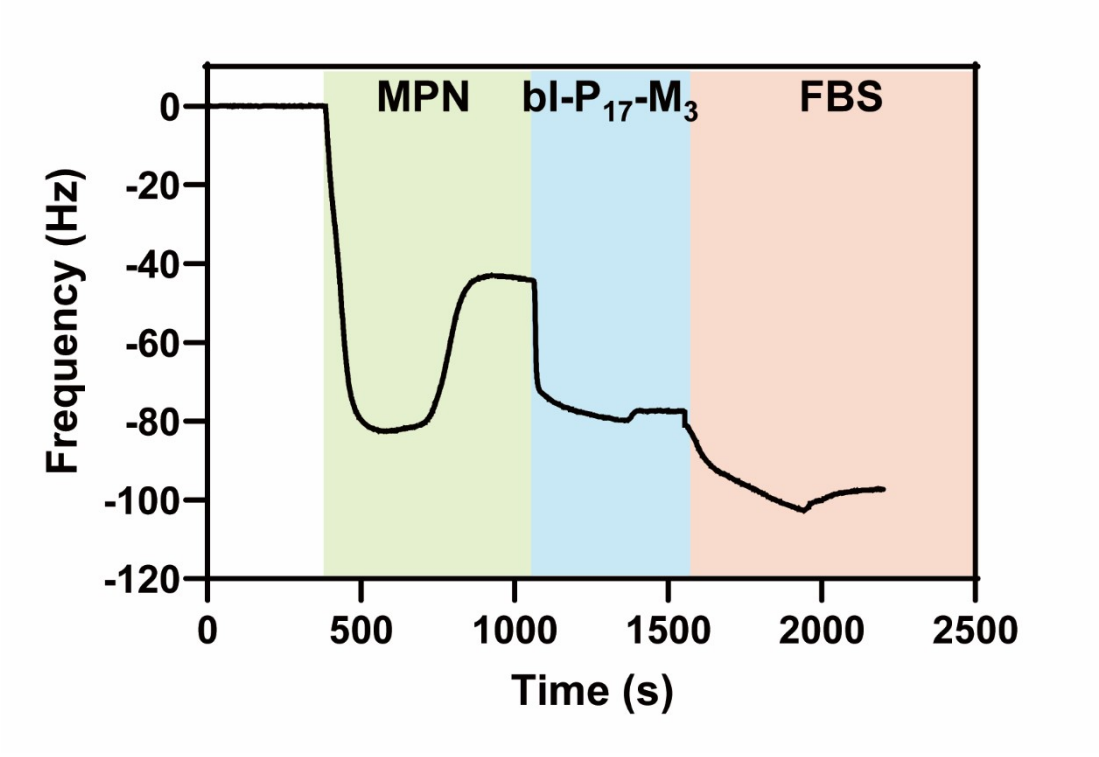

Figure S29. QCM-D frequency changes of copolymer modified Au substrates after FBS adsorption of bl-P_{17}-M_3.

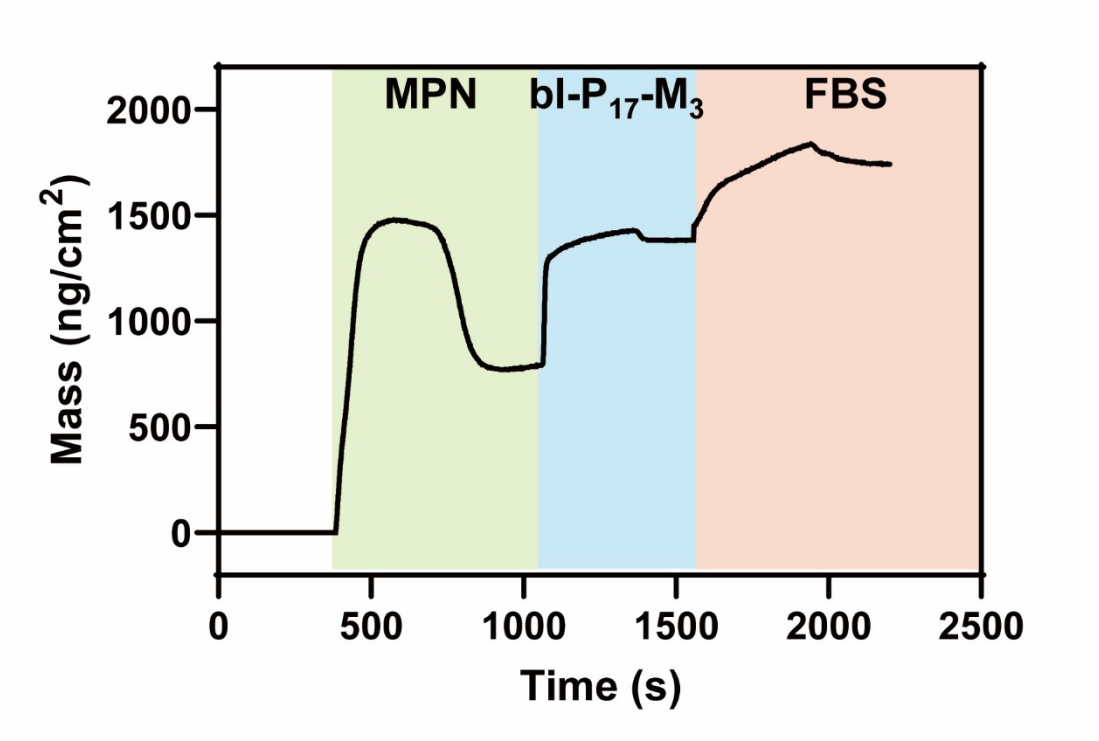

Figure S30. QCM-D mass changes of copolymer modified Au substrates after FBS adsorption of bl-P_{17}-M_3.

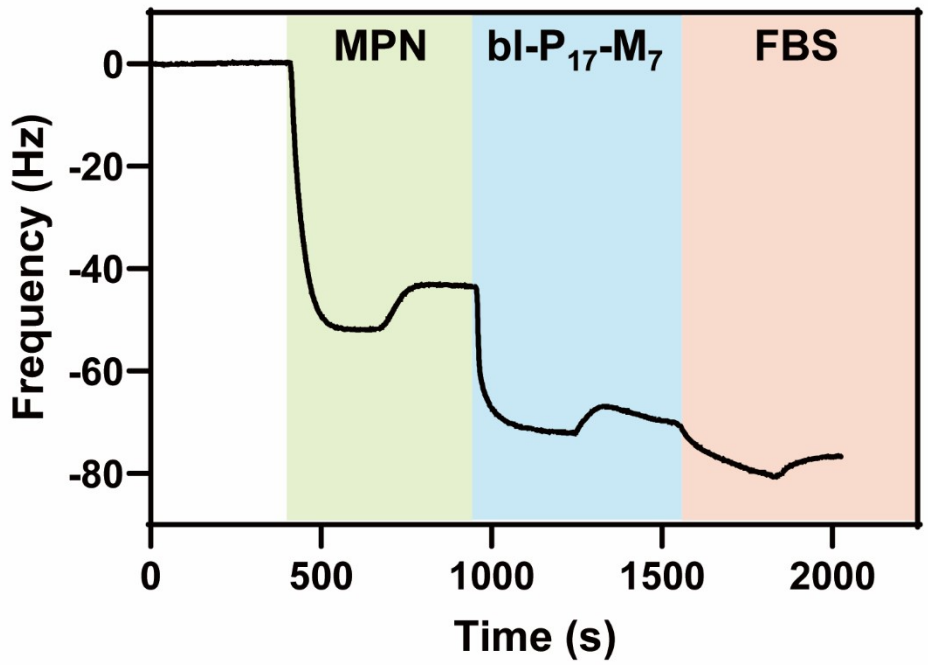

Figure S31. QCM-D frequency changes of copolymer modified Au substrates after FBS adsorption of bl-P_{17}-M_7.

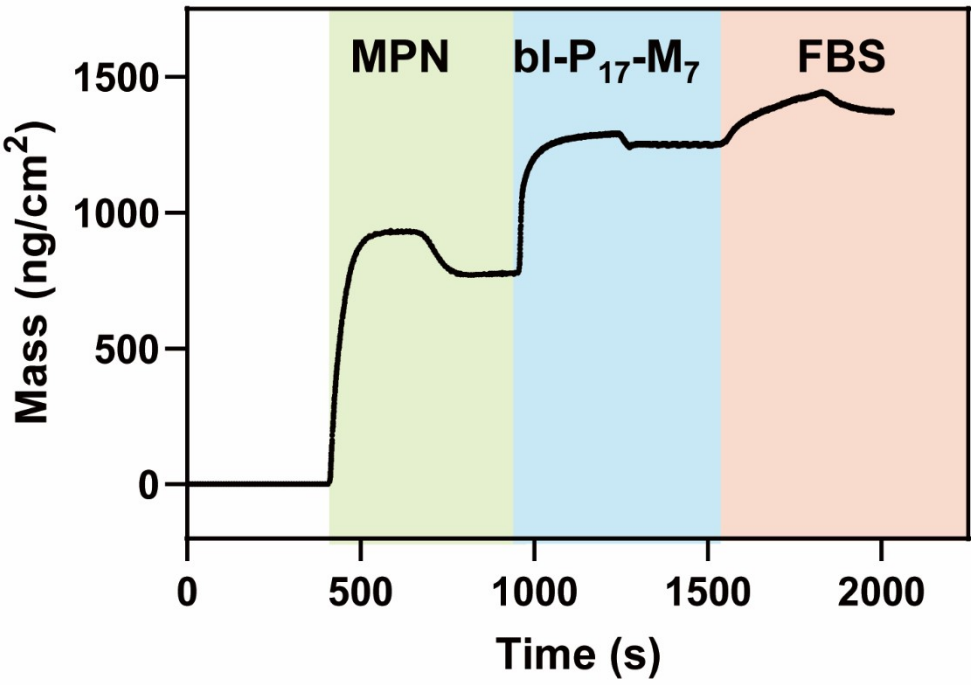

Figure S32. QCM-D mass changes of copolymer modified Au substrates after FBS adsorption of bl-P_{17}-M_7.

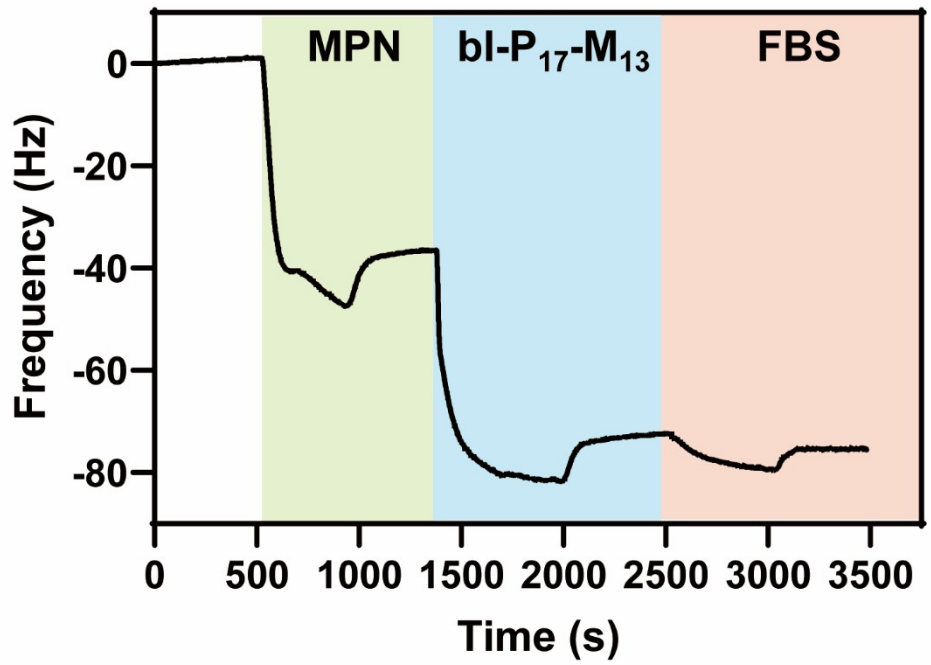

Figure S33. QCM-D frequency changes of copolymer modified Au substrates after FBS adsorption of bl-P_{17}-M_{13}.

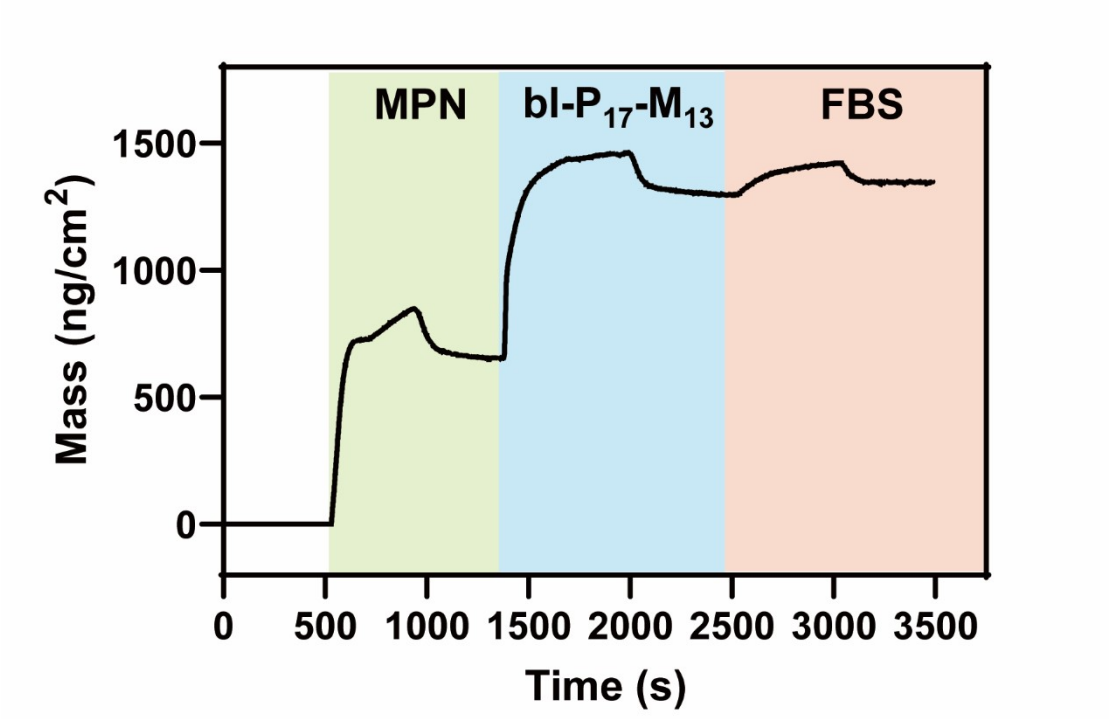

Figure S34. QCM-D mass changes of copolymer modified Au substrates after FBS adsorption of bl-P_{17}-M_{13}.

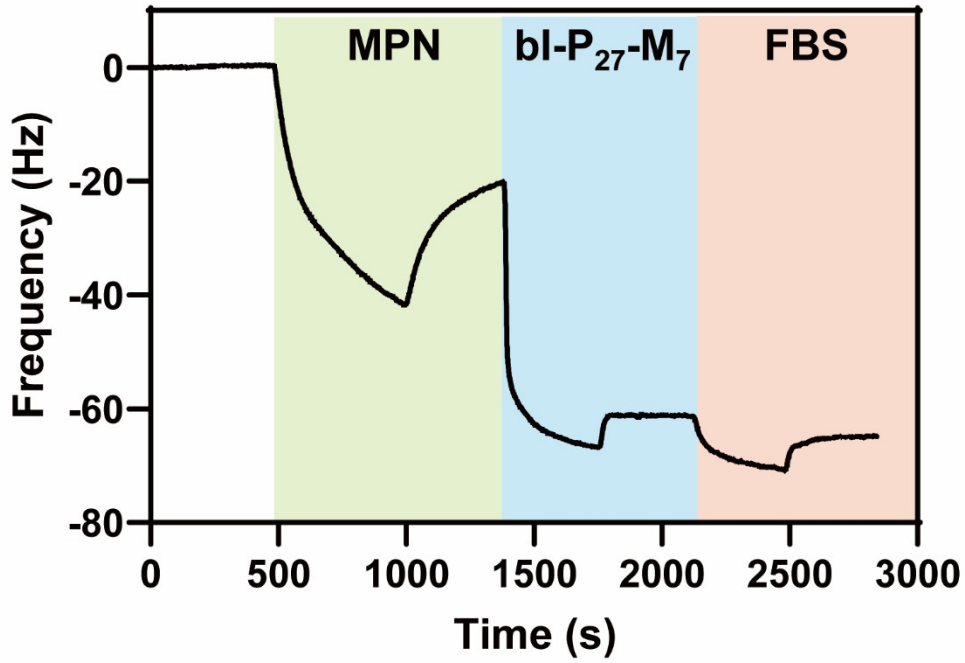

Figure S35. QCM-D frequency changes of copolymer modified Au substrates after FBS adsorption of bl-P_{27}-M_7.

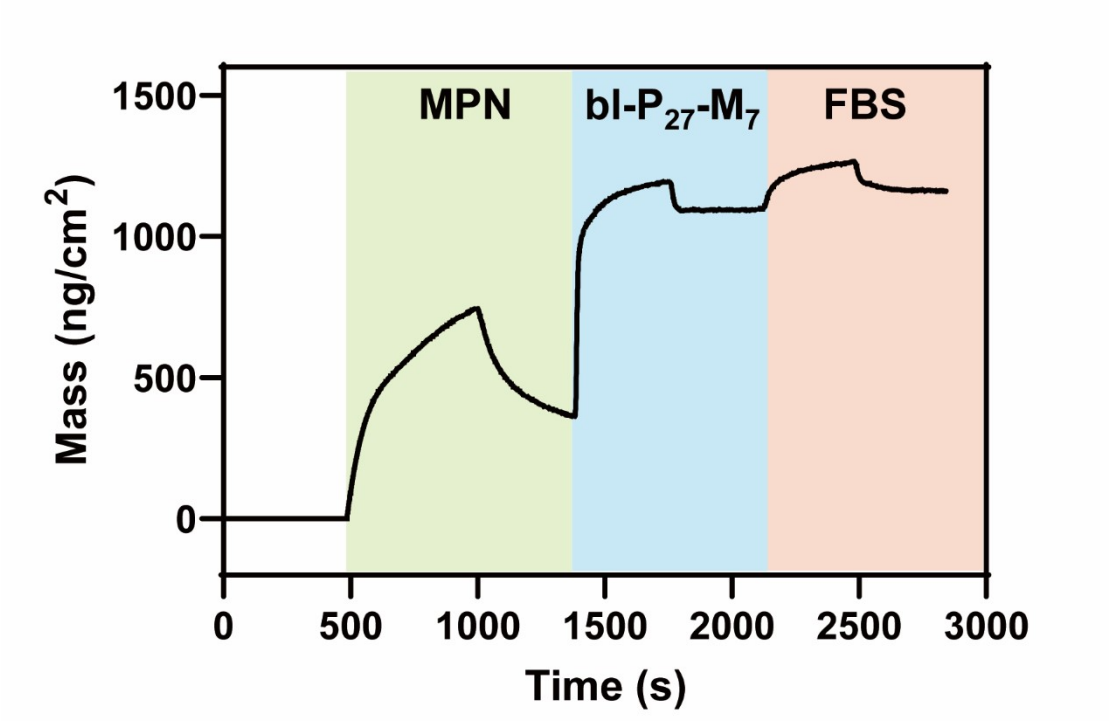

Figure S36. QCM-D mass changes of copolymer modified Au substrates after FBS adsorption of bl-P_{27}-M_7.

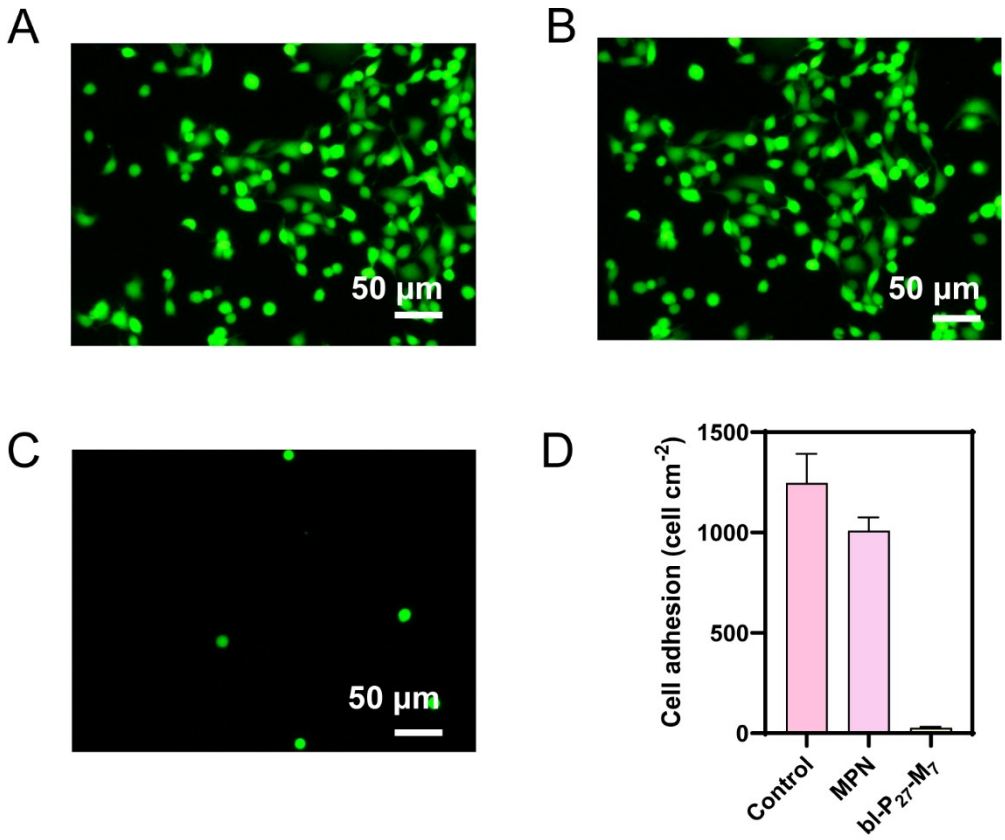

Figure S37. Representative fluorescence microscopy images of HUVEC cells adhered onto (A) Control, (B) MPN, (C) bl-P_{27}-M_7 modified substrates after 4 h of cell culture slides incubation. (D) Quantitative densities of adhered HUVEC cells. Data represent the mean ± SD (n = 5).

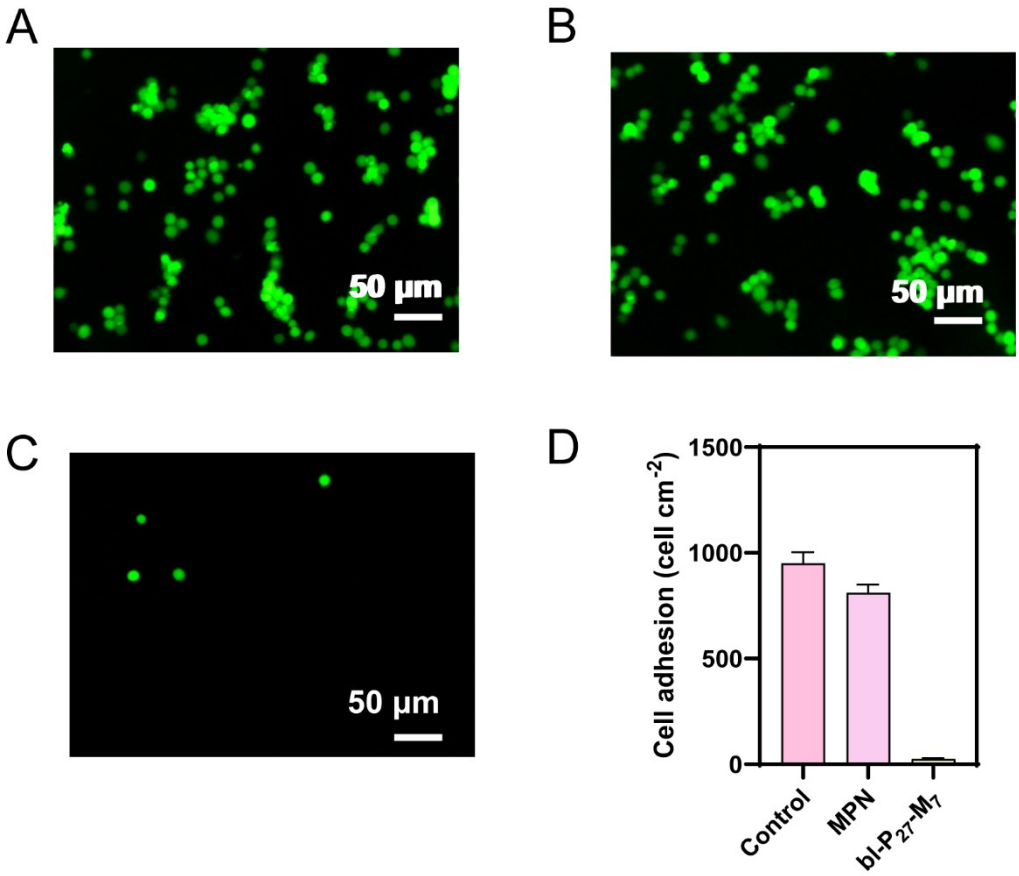

Figure S38. Representative fluorescence microscopy images of HUVEC cells adhered onto (A) Control, (B) MPN, (C) bl-P_{27}-M_7 modified substrates after 4 h of quartz slides incubation. (D) Quantitative densities of adhered HUVEC cells. Data represent the mean ± SD (n = 5).

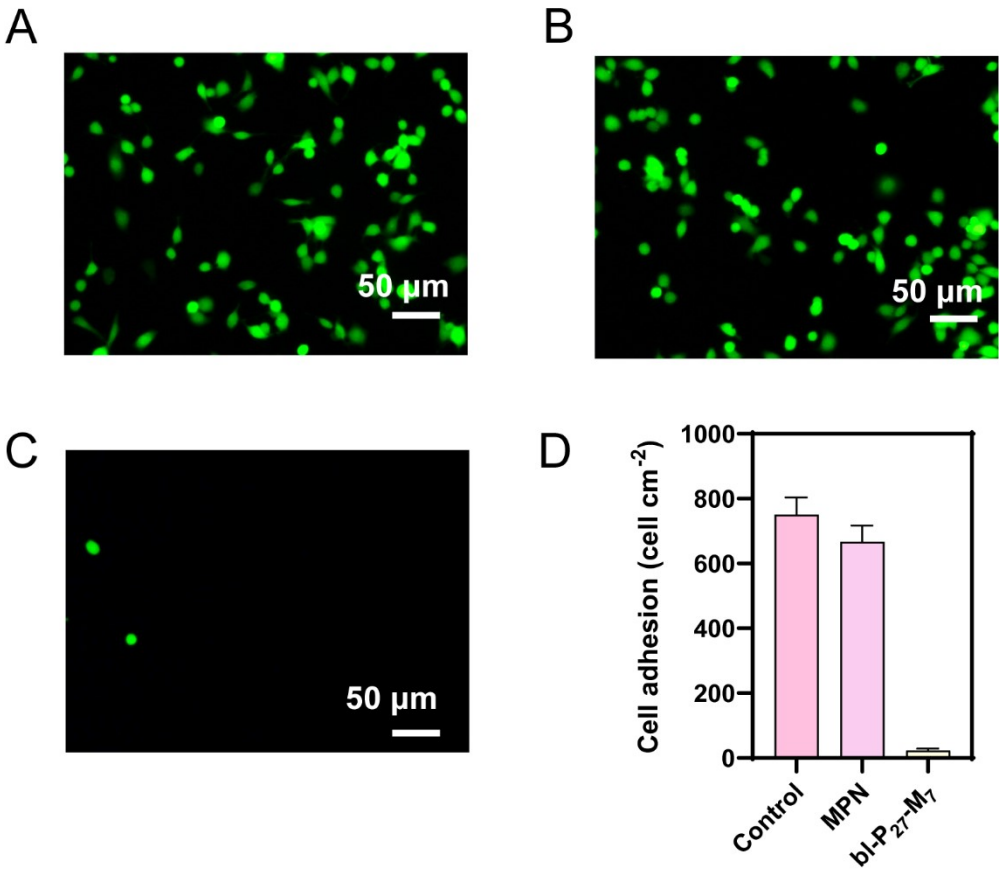

Figure S39. Representative fluorescence microscopy images of HUVEC cells adhered onto (A) Control, (B) MPN, (C) bl-P_{27}-M_7 modified substrates after 4 h of polymethyl methacrylate (PMMA) slides incubation. (D) Quantitative densities of adhered HUVEC cells. Data represent the mean ± SD (n = 5).

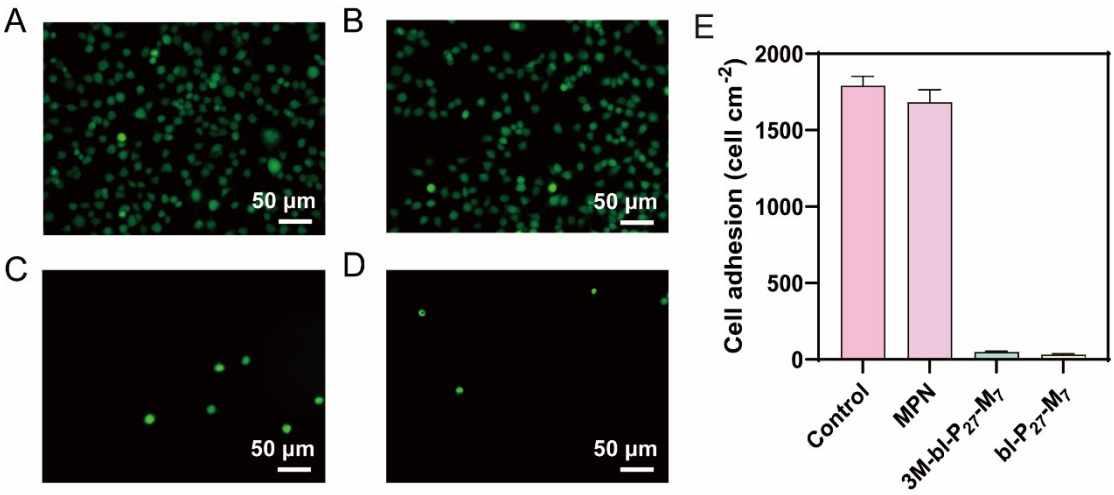

Figure S40. Representative IFM images of HUVEC cells adhered onto (A) Control, (B) MPN, (C) bl-P_{27}-M_7 after adhesion with 3M tape and (D) bl-P_{27}-M_7 modified substrates. (E) Densities of adhered HUVEC cells. Data represent the mean ± SD (n = 5).

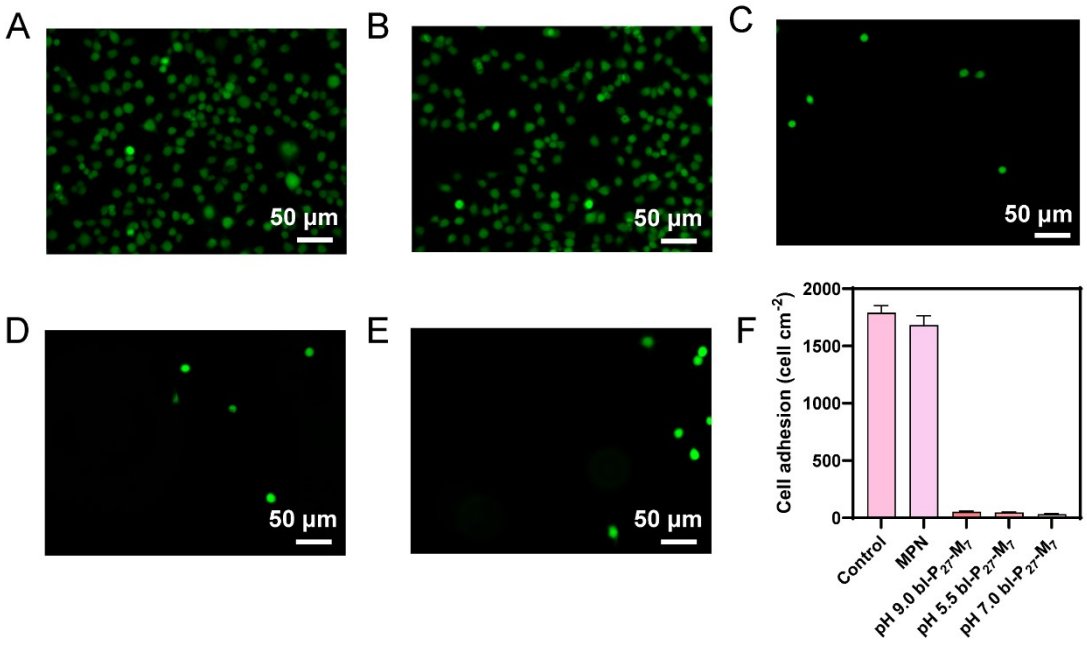

Figure S41. Representative IFM images of HUVEC cells adhered onto (A) Control, (B) MPN, (C) bl-P_{27}-M_7 modified substrates after co-cultivation in PBS solution with pH 5.5, (D) pH 7.0, and (E) pH 9.0 modified substrates. (F) Densities of adhered HUVEC cells. Data represent the mean ± SD (n = 5).

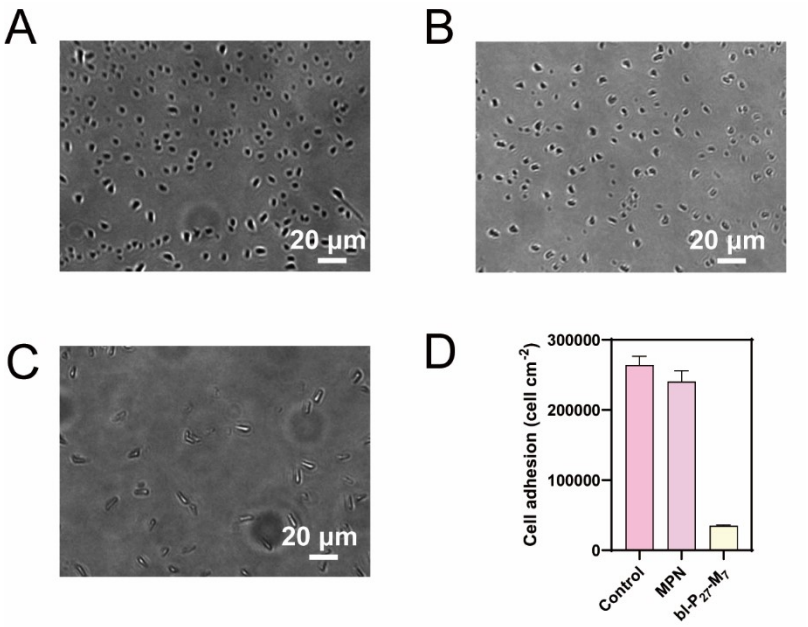

Figure S42. Representative microscope images of platelets adhered onto (A) Control, (B) MPN, (C) bl-P_{27}-M_7 modified substrates. (D) Densities of adhered platelets Data represent the mean ± SD (n =5)